

Weak Gravitational Lensing: Current Status and Future Prospects

NICK KAISER

Anglo-Australian Observatory
PO Box 296, Epping, NSW 2121, Australia
On Leave from CITA, University of Toronto
e-mail: kaiser@cita.utoronto.ca

August 25, 2018

Abstract

In this review I will describe progress that has been made in determining masses of galaxy clusters using ‘weak lensing’ and how this technique may be applied in the future to determine the dark matter distribution both on supercluster scales and on the scale of galaxy haloes.

1 Introduction

Masses of galaxy clusters have traditionally been obtained either from measurements of the velocity dispersion of the galaxies or from the temperature of the X-ray emitting gas, and have given a great deal of input to cosmology: These results have shown that the total cluster mass greatly exceeds the mass in galaxies and (for any reasonable Hubble constant) the mass in X-ray emitting gas, and thus suggest the existence of non-baryonic dark matter. They have been used to estimate the density parameter under the assumption that the mass-to-light ratio of clusters is equal to that of the universe as a whole, and, more recently, under the assumption that the baryonic-to-total mass ratio is representative of the universal value. They have also been used to try to estimate the cluster mass function, which potentially has much power to constrain theories for structure formation.

While vital for cosmology, these mass estimates are subject to a number of systematic uncertainties arising from the assumptions that go into the modelling, and which are rather hard to quantify. For the virial analysis, one must make assumptions about the anisotropy of the orbits, one typically assumes that light traces the mass; that the cluster is spherical, and one assumes that the cluster is dynamically relaxed. Similar assumptions go into the X-ray analysis,

yet it is not entirely clear to what extent these assumptions are valid, or what effect departures from sphericity etc. have on the mass estimates. Furthermore, any mass estimates made assuming equilibrium conditions must inevitably break down at radii $> 1 - 2h^{-1}\text{Mpc}$ outside of which material is falling into the cluster for the first time. Comparison of X-ray and virial mass estimates (e.g. Lubin and Bahcall 1993) show a general correlation, which is encouraging, but also show a large scatter on a case by case basis even for well observed clusters, which presumably reflects the breakdown of one or more of these assumptions.

In contrast, distortion of faint galaxies by the gravitational lens effect can yield a direct measurement of the 2-dimensional projected mass density with no assumptions about the dynamical state of the cluster whatsoever. Moreover, this technique is applicable at all radii (and the signal-to-noise is roughly independent of radius over a wide range of radii for reasonable models for the mass distribution). For the most massive clusters, this method gives masses to a precision of better than 20%, with somewhat higher precision possible with deeper observations, and promises to give a very powerful direct measurement of the mass distribution on supercluster scales; around bright galaxies; and can also provide powerful constraints on the redshift distribution of very faint galaxies.

2 Quantitative Cluster Mass Estimation

The effect of a foreground mass concentration along the line of sight is to map the surface brightness of distant background objects according to

$$f_{\text{obs}}(\vec{r}) = f_{\text{true}}(\vec{r} - \vec{\nabla}\phi) \quad (1)$$

where ϕ is the 2-D dimensionless surface potential which is related to the surface density by

$$\nabla^2\phi = 2\kappa \quad (2)$$

where $\kappa \equiv \Sigma/\Sigma_{\text{crit}}$. If we measure angular position relative to the centre of some galaxy, then its surface brightness will be distorted according to

$$f_{\text{obs}}(\vec{r}) = f_{\text{true}}(\Psi_{ij}r_j) \quad (3)$$

where the distortion or amplification tensor is

$$\Psi_{ij} = \delta_{ij} - \partial^2\phi/\partial r_i\partial r_j \quad (4)$$

which is a symmetric 2×2 tensor. The effect of a gravitational lens is to introduce a spatially coherent distortion of faint background galaxies. At small radii the distortion is strong and results in prominent ‘giant arcs’. At larger radii the distortion is weak, but may still be detected as a statistical anisotropy of the galaxy shapes. There are several steps in the process of obtaining a quantitative mass estimate for a cluster: First one must obtain high-quality

deep photometric data (preferably with multi-colour information), one must then apply some object finding algorithm to identify the galaxies and then construct some statistic which is sensitive to the polarisation of the shapes of the background galaxies. The next step is to calibrate the relation between the observed polarisation and the gravitational shear (this depends on the seeing which will tend to reduce the apparent polarisation of small objects). It is then usually necessary to correct for anisotropy of the instrumental point-spread-function (PSF) as this can easily introduce spurious polarisation of the faint galaxies. At this point one has a noisy 2-dimensional map of the shear field (or rather a set of noisy estimates of the shear — one for each background galaxy), and the next step is to invert this shear field to obtain the dimensionless surface density $\kappa = \Sigma/\Sigma_{\text{crit}}$. The final step is to estimate the critical surface density Σ_{crit} and thereby obtain the physical 2-dimensional surface density $\Sigma(\vec{r})$.

2.1 Shear Measurement

The most commonly used analysis software is the FOCAS package (Jarvis and Tyson, 1981) which identifies connected regions lying above some isophotal threshold (and attempts to split up overlapping galaxy images). This package calculates a variety of statistics, including intensity weighted second central moments $I_{ij} = \int d^2r r_i r_j f(\vec{r})$, from which one can form a ‘polarisation vector’ $\vec{e} = \{(I_{11} - I_{22}), 2I_{12}\}/(I_{11} + I_{22})$ whose expectation value one can show is proportional to the shear $\vec{\gamma} = \{(\phi_{,11} - \phi_{,22})/2, \phi_{,12}\}$. We have developed an alternative, though rather similar, system (described in Kaiser, Broadhurst and Squires, 1995; hereafter KSB) which, rather than using an isophotal threshold, smooths an image with a hierarchy of smoothing kernels and then identifies objects as local peaks of the significance as a function of position and smoothing radius. Our polarisation is defined similarly, but using second central moments calculated with a gaussian radial weight function with scale length matched to the size of the galaxy in order to minimise the noise from photon counting statistics. Another variant is that of Bonnet and Mellier (1994) who use the square root of the determinant of I_{ij} in the denominator in the definition of the polarisation instead of the trace $I_{11} + I_{22}$. The common feature of these methods is that in the absence of lensing, the expectation value of the polarisation should vanish by symmetry and a coherent shear will introduce a shift in the mean proportional to γ .

A variety of techniques have been applied to calibrate the relation between \vec{e} and $\vec{\gamma}$. The basic idea is to figure out how the polarisation values for a set of galaxies change under the influence of an applied shear. The complication is that the shear is applied before the smearing of the image by the seeing disk, but a number of methods have been developed to solve this problem. One approach (Tyson and Fisher 1995) is to model the properties of the faint galaxies, and then to generate synthetic images which are sheared by a known amount and then degraded to mimic the ground based conditions and then analysed. A somewhat

more direct approach (KSB) is to take deep HST images of small patches of sky and process these in a similar manner. While the amount of deep photometry is rather limited at the moment, such experiments show that relation between the shear and polarisation is approximately linear, and determine the constant of proportionality to about 10% fractional error. These experiments also allow one to optimise various features of the analysis to give robust and low noise estimates of the shear. Another approach (Wilson, Cole and Frenk, 1995) is to deconvolve ground based images, shear them and then reconvolve with the seeing PSF, and they too find that, while the correction for seeing can be quite large, it can be estimated quite reliably. Yet another approach is to shear the post-seeing images — which is equivalent to shearing the images first and then smearing with a PSF which is slightly anisotropic — and then reconvolve with a small but highly anisotropic PSF designed to recircularise the stellar images. This problem has also been considered by Villumsen (1995).

In addition to the effect of gravity, the shapes of galaxies are distorted by any instrumental PSF anisotropy. Luckily, stars in our galaxy provide a convenient control sample with which we can measure the PSF (and provided the seeing is reasonably good it is relatively straightforward to separate a subsample of faint stars). If the PSF were constant, it would then be fairly straightforward to reconvolve the image with a small but highly anisotropic PSF designed to recircularise the stars and this would null out any instrumental effect on the background galaxies. In fact, the PSF usually tends to vary across the field, which makes implementing such a scheme rather difficult. An alternative which seems to work very well though is to calculate, for each object, how its polarisation value would respond to a given PSF anisotropy, and one can then use the polarisation of the stars to develop a model for the PSF as a function of position on the image and then apply an appropriate linearised correction to the galaxy polarisation values.

3 Direct Estimate of the Convergence

The steps outlined above provide one with a noisy estimate of the shear $(\phi_{,11} - \phi_{,22})/2$, from which one must then somehow reconstruct $\kappa = (\phi_{,11} + \phi_{,22})/2$ by one of the techniques discussed below. It would be much simpler if one could measure the convergence directly. This is possible in principle, but somewhat difficult in practice using only photometric observations at least. The convergence will brighten and enlarge the faint galaxies (Broadhurst, Taylor and Peacock, 1995; Bartelmann and Narayan, 1995). If galaxies had a standard apparent luminosity or standard apparent size one could then readily determine κ directly. Unfortunately there is a wide distribution in the apparent sizes, the slope of the faint counts is such that the ‘amplification bias factor’ nearly vanishes, and experiments we have performed using deep HST data similar to those described above show that there is very little hope of obtaining useful cluster

mass estimates in this way.

A more promising approach has been suggested by Broadhurst (1995) who has shown that since the very red galaxies have a rather flat counts slope — this reflects the fact that as one goes fainter the galaxies tend to become bluer — they have a non-negligible (actually negative) amplification bias and so a cluster will tend to produce a depression in the counts of such background galaxies. The method does indeed seem to work, but tends to be noisier than the shear method due to the rather low number density of very red galaxies and also the fact that these galaxies are clustered. However, it does provide a useful check on the results of the shear analysis, and also removes an ambiguity in shear based mass reconstructions.

4 Reconstruction Methods

For weak lensing, the desired surface density κ and the observed shear $\vec{\gamma}$ are all expressed as second derivatives of the surface potential:

$$\begin{aligned}\kappa &= (\phi_{,11} + \phi_{,22})/2 \\ \gamma_1 &= (\phi_{,11} - \phi_{,22})/2 \\ \gamma_2 &= \phi_{,12}\end{aligned}\tag{5}$$

One can simply fourier transform these equations to obtain algebraic relations between $\tilde{\kappa}$, $\tilde{\gamma}_1$, $\tilde{\gamma}_2$. These allow one to recover $\tilde{\kappa}$ from either $\tilde{\gamma}_1$ or $\tilde{\gamma}_2$ alone (though with particularly bad noise for certain wave-vectors), and the optimally weighted combination is

$$\tilde{\kappa} = (\hat{k}_1^2 - \hat{k}_2^2)\tilde{\gamma}_1 + 2\hat{k}_1\hat{k}_2\tilde{\gamma}_2\tag{6}$$

which has a flat noise power spectrum. On inverse fourier transforming this gives an estimate of κ as a convolution of the shear with a particular kernel:

$$\kappa(\vec{r}) = \int d^2r' K_\alpha(\vec{r} - \vec{r}')\gamma_\alpha(\vec{r}')\tag{7}$$

(Kaiser and Squires 1993). Simulations (e.g. Wilson et al., 1995) show that this works quite well, but there are some limitations. The kernel derived above falls asymptotically as $1/r^2$ at large radii, and thus, strictly speaking, requires data extending to infinity. With finite data this results in a bias in the outer parts of the reconstruction as illustrated in figure 1. Another limitation is that the result is limited to the weak regime. There has been considerable progress recently in addressing both of these limitations.

One way to solve the bias problem (Kaiser, 1995) is to exploit the local expression for the gradient of κ in terms of the gradient of the shear:

$$\vec{\nabla}\kappa = \begin{bmatrix} \partial\kappa/\partial x \\ \partial\kappa/\partial y \end{bmatrix} = \begin{bmatrix} \partial\gamma_1/\partial x + \partial\gamma_2/\partial y \\ \partial\gamma_2/\partial x - \partial\gamma_1/\partial y \end{bmatrix}\tag{8}$$

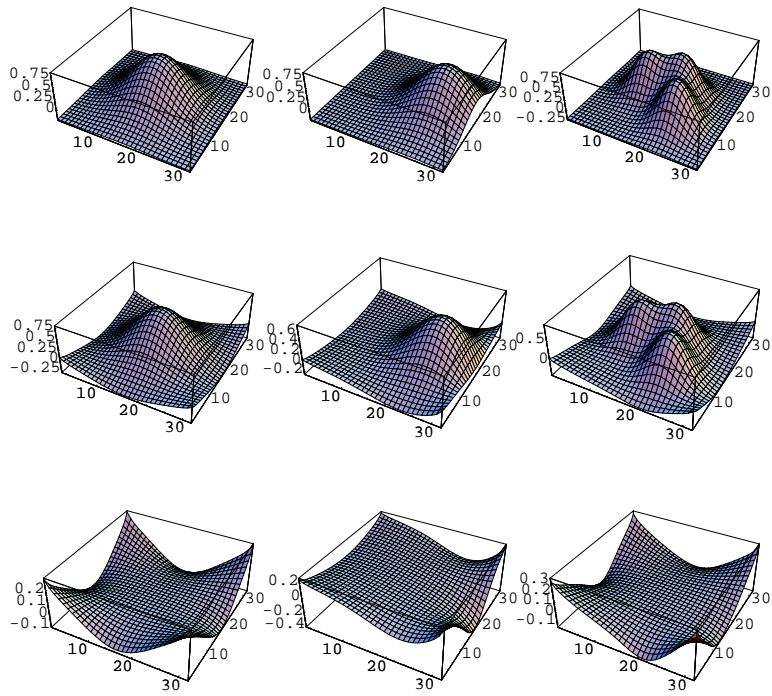


Figure 1: Illustration of the bias in the Kaiser-Squires '93 method. The top row of panels show three input model lenses; the middle panels show the reconstructions, and the bottom row of panels show the residuals with an expanded vertical scale.

which follows directly from the relations between κ , $\bar{\gamma}$ and ϕ . This tells us that in principle at least κ is fully determined up to a constant, and there are many ways one can determine the surface density at some point relative to its value averaged over some control region by averaging over line integrals (Seitz and Schneider, 1995; Schneider, 1995; Kaiser *et al.*, 1995). There are other ways to remove the bias. It is possible to construct FFT based methods which are unbiased, but a detailed comparison of such techniques (Squires and Kaiser, 1995) reveals that all of the methods so far considered result in somewhat higher noise in the long-wavelength components (which is unfortunate since the bias only affects the long wavelengths).

Our currently preferred approach is a regularised maximum likelihood method (Squires and Kaiser, 1995). What we do is to model the surface density as a sum of discrete fourier modes, but on a box which extends beyond the region where we have data (this is necessary if one wants the reconstruction to be unbiased). We can then form the likelihood $P(\text{data}|\text{model})$ and one could determine the fourier amplitudes which maximise this. If one has many modes (i.e. good high frequency resolution) this is unstable, and a certain combination of modes tends to blow up. Instead what we do is to apply a regularisation by minimising $P(\text{data}|\text{model}, \text{prior})$ where the prior model is that the mode amplitudes are drawn from gaussian distributions with variance $P = \text{constant}$. This very similar to “classic” maximum entropy and is quite simple to calculate. Now this suffers from the usual problem with this type of technique that the result tends to be biased downwards if P is set to be too small. However, we have found that in practice one only needs a very mild regularisation (i.e. large P) to suppress the unstable modes and for a wide range of P -values one obtains a stable and robust reconstruction. It must be admitted though that the results, as with many of the unbiased estimators we have explored, is rather hard to distinguish from the original biased method.

4.1 Aperture Densitometry

The 2-dimensional reconstructions are very nice for some purposes: it is interesting to compare morphology of the mass and light distribution, and the fact that the peak of the mass reconstructions coincides with the centroid of the light gives one some confidence in the method. However, if one is interested only in the radial mass profile (or if one simply wants an estimate of the mass within some radius) then an alternative approach is to use aperture densitometry. The basis for this method is a identity between the mean tangential shear $\langle \gamma_t \rangle$ taken around a circular loop and the derivative of the mean surface density within the loop $\bar{\kappa}$ wrt loop radius:

$$\langle \gamma_t \rangle = \frac{1}{2} \frac{d\bar{\kappa}}{d \ln r} \quad (9)$$

Integrating this wrt $\ln r$ gives an expression for $\bar{\kappa}$ within some aperture of radius r_1 relative to the mean of κ in some surrounding annulus $r_1 < r < r_2$:

$$\bar{\kappa}(< r_1) - \bar{\kappa}(r_1 < r < r_2) = \zeta(r_1, r_2) \equiv \frac{2}{(1 - r_1^2/r_2^2)} \int_{r_1}^{r_2} d \ln r \langle \gamma_t \rangle \quad (10)$$

which can then be simply estimated as a sum over the individual galaxy shear estimates. A nice feature of this method is that the result depends only on data outside the aperture, so this can be chosen to minimise problems with non-linearity and contamination by cluster members. Another advantage of this approach (over simply measuring the mass excess from a 2-D reconstruction say) is that one obtains a simple yet rigorous estimate of the uncertainty. This technique was first applied by Fahlman *et al.*, (1994), and has also been used by Tyson and Fisher, 1995 in their analysis of A1689.

If one takes r_2 to be the outer boundary of the data then one can plot ζ vs. r_1 , and thus obtain a lower bound on the mass profile. One can also compare this with the analogous quantity calculated for the surface brightness and thereby compare the mass and light profiles directly. However, one should bear in mind that that this is then a cumulative statistic, so the errors at different radii are strongly correlated.

A nice feature of this kind of analysis is that if one applies a ‘rotation’ $\gamma_1 \rightarrow \gamma_2$, $\gamma_2 \rightarrow -\gamma_1$ to the shear estimates then any real signal should vanish. This provides a very useful check on artifacts, or the possibility of spurious shear arising from intrinsically correlated ellipticities.

4.2 Non-Linear Reconstruction

There have been some advances in extending the 2-dimensional mass reconstruction techniques into the non-linear regime. If one only uses the information encoded in the shapes of galaxies, then all one can hope to learn from observations on some patch of sky is the ratio and orientation of the eigenvalues of the distortion tensor Ψ_{ij} . Now since $\Psi_{11} = 1 - \kappa - \gamma$, $\Psi_{22} = 1 - \kappa + \gamma$, it follows that Ψ_{22}/Ψ_{11} is only a function of the combination $\gamma/(1 - \kappa)$. Furthermore, we can only observe the modulus of the ratio of eigenvalues, whereas the actual ratio flips sign if we cross a critical line. The upshot of all this is that one can define an observable polarisation $e = (1 - R)/(1 + R)$ where R is the ratio of the smaller to the larger (in magnitude) eigenvalue, which in the general coordinate frame becomes a vector relation, and which in the even parity regime is equal to $\gamma/(1 - \kappa)$ while in the odd parity regime is equal to $(1 - \kappa)/\gamma$. This apparent ambiguity has been dubbed by Schneider and Seitz (1995) a ‘local invariance transformation’.

Now using the expression above for the gradient of κ in terms of $\partial\gamma_i/\partial r_j$ it is not difficult to derive an explicit expression for the gradient of the log of $1 - \kappa$

in terms of the observable polarisation \vec{e} .

$$\vec{\nabla} \log(1 - \kappa) \equiv \vec{u} = \begin{bmatrix} 1 + e_1 & e_2 \\ e_2 & 1 - e_1 \end{bmatrix} \begin{bmatrix} \partial_x & \partial_y \\ -\partial_y & \partial_x \end{bmatrix} \begin{bmatrix} e_1 \\ e_2 \end{bmatrix} \quad (11)$$

(Kaiser, 1995). This is for the even parity region; in the odd parity region we must use $e = (1 + R)/(1 - R)$. This expression makes explicit a further ambiguity in non-linear reconstruction (Schneider and Seitz’s ‘global invariance transformation’): that one can always multiply $1 - \kappa$ by some arbitrary constant without changing the distortion. This is not much of a problem if one has data extending to large distance, since the ‘wrong’ choice of constant will give κ tending to a non-zero constant at large radii and will therefore give a mass diverging as r^2 . It also shows that the local invariance transformation ambiguity can be resolved: Simply calculate the curl of the vector \vec{u} ; this should of course vanish, but will only do so in general if one is using the appropriate expression for \vec{e} .

The main practical difficulty we have found in applying this to real data is contamination of the faint galaxy population by cluster galaxies in the central parts of the cluster.

5 Determining the Critical Surface Density

The above methods allow one to determine κ , the dimensionless surface density. In order to obtain the physical surface density one must multiply by Σ_{crit} which depends on the redshift distribution for the faint galaxies. Now for a single screen of sources, and assuming a Einstein - de Sitter universe, the critical surface density is $\Sigma_{\text{crit}} = (4\pi a_l w_l \max(1 - w_l/w_s, 0))^{-1}$, where comoving distance $w = 1 - 1/\sqrt{1+z}$. In general, if we average over galaxies with some distribution of redshifts we must use the $\Sigma_{\text{crit, effective}} = 1/\langle 1/\Sigma_{\text{crit}} \rangle$ in place of Σ_{crit} . The big problem is that the redshift distribution is rather poorly known (the deepest complete surveys only reach magnitudes $I \simeq 22$ (Lilly *et al.*, 1995), whereas the typical lensing observations go 2 or more magnitudes deeper. Now for low redshift lenses, $z_l \sim 0.2$, the effective critical surface density is very weakly dependent on $n(z)$ and the uncertainty in determining Σ_{crit} is very small ($\sim 10\%$). However, for more distant clusters (and for some of the other applications described below) $n(z)$ is a big issue.

In some of our cluster observations we can detect the shear for galaxies in the magnitude range where redshifts are available, albeit with less precision than if we use all the galaxies, and by comparing with the shear strength observed for the fainter samples we can constrain $n(z)$ at fainter magnitudes. With only one cluster, this is rather noisy, but if one had a sample of say 10 or so massive clusters at the same redshift then one can hope to constrain $n(z)$ for faint galaxies quite well, and thus tighten up the normalisation of the absolute mass scale. By studying cluster lenses at a range of redshifts one can hope

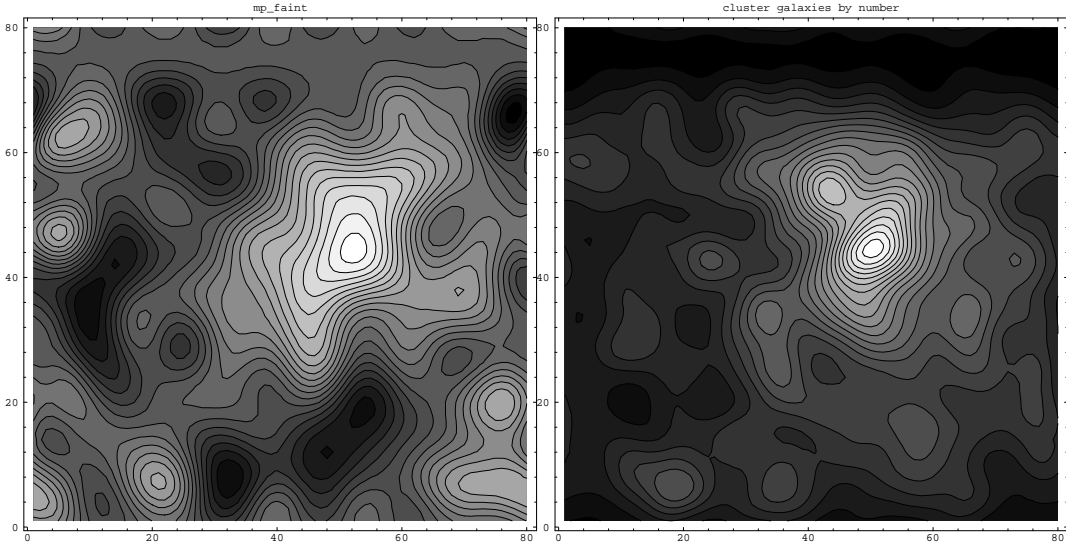


Figure 2: The left panel shows the reconstruction of the surface mass density for A1689 made using the ‘regularised maximum likelihood’ method. The panel on the right shows the surface number density of cluster galaxies. The side of the box is $\sim 8'$ or about $1h^{-1}\text{Mpc}$ at the redshift of the cluster.

to build up a fairly detailed picture of $n(z; m)$; this, rather than cluster mass estimation, has been the primary goal of the Durham group (Smail *et al.*, 1995), who targeted relatively high- z clusters, and the idea has been discussed by Bartelmann and Narayan (1995). An exciting, if somewhat distant, prospect is that if one could obtain complete samples of spectroscopic redshifts at these magnitudes then by comparing with the lens inferred estimates (which really measure the relative comoving distance distributions), one might be able to constrain the cosmological world model.

6 Results for Clusters

The 2-dimensional surface density reconstruction for A1689 is shown in figure 2 along with the projected density of cluster galaxies. The peaks of the mass

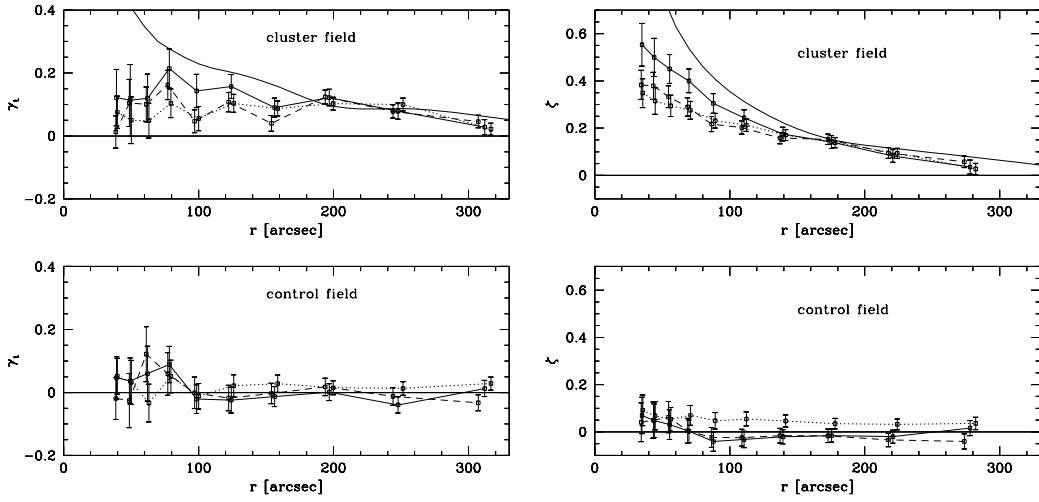


Figure 3: A1689 tangential shear profile is shown on the left. Upper plot shows the tangential shear profile with V-band dotted, I-band dashed and the color selected sample solid. The smooth solid line is the predicted shear for a mass-to-light ratio of $450h$ as inferred from the giant arc. Lower plot shows same for control field. The ζ statistic used for calculating mass within an aperture is shown on the right (beware that the errorbars in ζ are correlated).

and light coincide very well indeed and there seems to be some similarity in the morphology of the mass and light distributions. The data used here were taken by Tom Broadhurst at the NTT and comprise about 3 hrs net integration in both V and I passbands. He also observed a control field which gives a useful check on the reliability of the analysis.

A more quantitative picture of the shear profile is shown in figure 3. These figures show that the shear is measurable repeatably in both passbands, and that the strength of the shear at large radii agrees with that predicted for a mass-to-light ratio of about $450 h$ in solar units. (Tyson and Fisher found essentially the same value, though their calibration involved modelling of the faint galaxy population rather than degraded HST images as used here). It is encouraging that no significant shear is found in the control field. Closer to the cluster centre, the measured shear is much smaller than that predicted. This is largely due to contamination by cluster members. The solid line with errorbars shows the result of removing galaxies which lie in the conspicuous horizontal sequence on the colour-magnitude diagram. This increases the shear substantially; the residual discrepancy may be due to the mass having a somewhat flatter profile than the cluster galaxies, but it may also be due to bluer cluster members we have failed to remove.

We have performed a similar analysis on A2218 (Squires, *et al.*, 1995), and obtain a similar mass-to-light ratio, though with somewhat larger ($\sim 20\%$) statistical uncertainty (for A1689 the statistical error in the aperture mass is only about 10%, with a systematic error of about the same order arising from uncertainties in $n(z)$ etc.). The first cluster we applied this technique to, ms1224, gave a somewhat larger $M/L \simeq 800h$ (and a mass much larger than obtained by virial analysis). From early, but rather limited, data on A2163, the hottest X-ray cluster known, we found surprisingly little evidence for shear. We now have much more data on this cluster, but have yet to analyse it in detail.

Smail *et al.* 1995, have obtained broadly similar results for several clusters, obtaining $M/L \simeq 500h$, and the Toulouse group (Bonnet *et al.*, 1993; Bonnet *et al.*, 1994) also measured the weak shear field around Q2345+007 and in the cluster CL0024.

The mass-to-light ratios from weak lensing are somewhat larger than those typically obtained from X-ray or virial analysis (though as mentioned, in some cases the lensing mass falls below the other estimates). It is then natural to try to estimate Ω (under the usual, though obviously questionable assumption that the M/L for the cluster is that same as that for the universe as a whole). If one uses the estimates for the comoving luminosity density measured locally (e.g. Loveday *et al.*, 1992) then one infers $\Omega \simeq 0.3$. However, there are strong indications from recent fainter redshift surveys (Lilly *et al.*, 1995; Colless, 1995) that the comoving luminosity density is actually much higher, and then this exercise gives $\Omega \simeq 1$.

An interesting new approach is to target bright radio sources rather than cluster lenses (Fort *et al.*, 1995). The idea is that these very bright objects may

have been amplified by intervening matter. If so, and if the lensing structures lie at $z < 0.5$ or so, then one might be able to detect the shear due to the hypothetical lens on faint galaxies, and the data do indeed show the expected signal.

7 Future Prospects

This subject is currently undergoing a major boost in instrumentation. In the past the size of detectors has been very limited, and in order to measure the shear at large radii from the cluster centre has required painstakingly building up a mosaic of images. CFH has recently introduced MOCAM (a mosaic of 4 chips each the same size as the earlier 2048^2 FOCAM chip), and this will shortly be superseded by Luppino's mosaic of eight 2048×4096 chips which is 4 times larger still (Metzger, Luppino and Miyazaki, 1995). With these new instruments it will be possible to measure the shear in clusters to much larger radii and/or push deeper for better signal to noise. In addition several new possibilities open up.

One possibility is to use galaxy-galaxy lensing to constrain the profiles of dark haloes around galaxies. Individual bright galaxies with rotation speeds of $\simeq 200$ km/s are ~ 100 times weaker lenses than very massive clusters like A1689. As the latter was only detected at about the 10-sigma level, bright galaxies are clearly too weak to detect individually. However, by stacking the results for many foreground galaxies it may be possible to build up a statistical halo profile. This was originally tried by Tyson *et al.*(1984) using photographic plates. We have looked for the effect with our limited number of blank control fields etc. but, not too surprisingly, find a null detect as yet. There have been two recent claims to detect the effect: Brainerd *et al.*(1995), using a single $10'$ -square field taken at Palomar, and the MDS team have found the effect in HST images of the 'Groth Strip'. Both of these results are of fairly low statistical significance, but with much more extensive photometry that should now become feasible the situation should improve dramatically.

Another promising approach is to determine the power-spectrum of mass-fluctuations on supercluster scales. The first quantitative predictions of weak lensing by large-scale structure were made by Blandford *et al.*, 1991, and Miralda-Escude, 1991. The predictions are somewhat model dependent, but a shear at about the 1% level and coherent over degree scales seems inescapable. A nice way to analyse this kind of observations is to measure the 2-D power spectrum of the shear, which is then related in a rather simple and direct manner to the 3-D power spectrum of mass fluctuations $P(k)$ (Kaiser, 1992). Such a signal is well within reach: our individual cluster fields each give null results for the net shear at about the 1% level, but cover only small fraction of a square degree (see also Mould *et al.*, 1994; Villumsen, 1995). By increasing the field size it should prove possible to detect the effect at a high level of confidence on each

degree scale ‘pixel’ and thus put powerful constraints on theories for structure formation.

8 References

- Lubin, L., and Bahcall, N., 1993. *ApJ.*, 415, L17
Jarvis, J.F., and Tyson, J.A., 1981. *AJ*, 96, 476
Kaiser, N., Squires, G., and Broadhurst, T., 1995. *ApJ*, in press
Bonnet, H., and Mellier, Y., 1994. submitted to *A&A*
Tyson, J.A., and Fisher, P., 1995, *ApJ*, 446, L55
Wilson, G., Cole, S., and Frenk, C., 1995, preprint
Villumsen, J.V., 1995. preprint, astro-ph/9507007
Villumsen, J.V., 1995. preprint, astro-ph/9503011
Broadhurst, T., Taylor, A., and Peacock, J., 1995. *ApJ*, 438, 49
Bartelmann, M., and Narayan, R., 1995. *ApJ*, in press, astro-ph/9411048
Broadhurst, T., 1995. in proceedings “5th Maryland Dark Matter Meeting”, astro-ph/9505010
Kaiser, N., and Squires, G., 1993. *ApJ*, 404, 441
Kaiser, N., 1995. *ApJ*, 439, L1
Seitz, S., and Schneider, P., 1995. *A&A*, in press, astro-ph/9503096
Schneider, P., 1995. *A&A*, in press, astro-ph/9409063
Kaiser, N., Squires, G., Fahlman, G., Woods, D. and Broadhurst, T., 1995. In “Wide Field Spectroscopy and the Distant Universe”, proc. 35th Herstmonceux Conference, ed. S. Maddox, World Scientific
Squires, G., and Kaiser, N., 1995, in preparation
Fahlman, G., Kaiser, N., Squires, G., and Woods, D., 1994. *ApJ*, 437, 56
Schneider, P. and Seitz, C., 1995, *A&A*, 294, 411
Smail, I., Ellis, R.S., Fitchett, M.J. & Edge, A.C., 1995. *MNRAS*, 273, 277
Squires, G., Kaiser, N., Babul, A., Fahlman, G., Woods, D., Neumann, D., & Bohringer, H. 1995. To appear in the *ApJ*.
Bonnet, H., Fort, B., Kneib, J.-P., Mellier, Y., Soucail, G., 1993. *A&A*, 280, L7
Bonnet, H., Mellier, Y., Fort, B., 1994. *ApJ*, 427, L83
Loveday, J., Peterson, B., Efstathiou, G., and Maddox, S.J., 1992. *ApJ*, 390, 338
Lilly, S., Tresse, L., Hammer, F., Crampton, D., and Le Fevre, O., 1995. preprint, astro-ph/9507079
Colless, M., 1995. In “Wide Field Spectroscopy and the Distant Universe”, proc. 35th Herstmonceux Conference, ed. S. Maddox, World Scientific
Fort, B., Mellier, Y., Dantel-Fort, M., Bonnet, H., Kneib, J.-P.: 1995, preprint, astro-ph/9507076
Metzger, M., Luppino, G., and Miyazaki, S., 1995. preprint
Tyson, A., Valdes, F., Jarvis, J., and Mills, A., 1984. *ApJ*, 281, L59.
Brainerd, T., Blandford, R., and Smail, I., 1995. preprint, astro-ph/9504010

Blandford, R., Saust, A., Brainerd, T., and Villumsen, J., 1991. MNRAS, 251, 600
Miralda-Escude, J., 1991. ApJ, 380, 1
Kaiser, N., 1992. ApJ, 388, 272
Mould, J., Blandford, R., Villumsen, J., Brainerd, T., Smail, I. et al.: 1994, ApJ, 271, 31

